We are IntechOpen, the world's leading publisher of Open Access books
Built by scientists, for scientists

4,800
Open access books available

122,000
International authors and editors

135M
Downloads

Our authors are among the

154
Countries delivered to

TOP 1%
most cited scientists

12.2%
Contributors from top 500 universities

CLARIVATE ANALYTICS
BOOK CITATION INDEX
INDEXED

WEB OF SCIENCE™

Selection of our books indexed in the Book Citation Index
in Web of Science™ Core Collection (BKCI)

Interested in publishing with us?
Contact book.department@intechopen.com

Numbers displayed above are based on latest data collected.
For more information visit www.intechopen.com

Geohazards in the Fjords of Northern Patagonia, Chile

María-Victoria Soto, Pablo Sarricolea,

Sergio A. Sepúlveda, Misael Cabello, Ignacio Ibarra,

Constanza Molina and Michael Maerker

Additional information is available at the end of the chapter

Abstract

A geomorphological analysis of the Comau Fjord was carried out to identify geohazards that are a product of current landform dynamics and processes. The geological setting of the area includes fractured metamorphic and volcanic rocks forming steep hillslopes in an active tectonic context due to the Liquiñe-Ofqui Fault Zone (LOFZ). Geomorphological and hazard mapping was performed using aerial photographs, GIS geoprocessing and fieldwork in January and May 2016 and February 2017. The susceptibility of landsliding was statistically assessed and validated with the inventory of landslides completed during fieldwork. The triggering of geohazards such as landslides and fluvial floods in the study area is associated with high annual precipitation (>5000 mm annually) with a concentration of rainfall that has increased in the last 50 years. Geohazard mapping demonstrated the potential for rock and earth falls, debris flows and river floods, as well as the potential impact of these geohazards on the area's intensive aquaculture industry and a main national highway projected for the eastern flank of the fjord. In a geographical scenario of environmental and territorial change, the present and future human occupation of Comau Fjord's coast constitutes potential hazard and risk conditions for aquaculture infrastructure and highway users.

Keywords: geohazard, North Patagonia, Comau Fjord, landslides, GIS

1. Introduction

Natural hazards are due to the interaction between environmental and social changes, and the patterns of land use associated with economic development and the processes of urbanization which increase people's exposure and vulnerability [1–6]. In such a context, natural risk is also considered to be an unresolved social problem [7].

Climate change scenarios are a new challenge for the study of natural hazards, risks and adaptation to hazards [8–11]. For example, during the period between 1900 and 2013, floods were the most frequent natural disaster, affecting more people than any other event of natural origin, [12], phenomena that intensively affected urban and rural areas alike [13].

Kappes et al. [14] suggest that the different types of hazards, scales of analysis, magnitudes of measures and risks constitute a scenario of multiple risks, which are also associated with environmental changes and human impact. Furthermore, human impact also functions as an agent of change in the processes and behavior of morphological systems [15].

Glacial and periglacial areas are geomorphological systems of high sensibility to climatic agents [16, 17] that are accentuated by the marine influence of the South Pacific Ocean. The climate changes modeled for the sector [18–21] that add future productive interventions particular to anthropic agents suggest an even more complex future for natural and territorial systems [22–24].

The most frequent natural hazards in mountainous environments are shallow landslides, associated with a landscape modeled by glacial and tectonic processes, such as those identified in the fjords of Norway [25–27]. Furthermore, large tsunamis from landslides have also been registered in Norway's fjords.

The purpose of this study is to establish the geomorphic conditions in the Comau Fjord, the associated natural hazards, and the impacts on vulnerable areas caused by these hazards, including the direct impact on a highway currently under construction and the potential population of the area.

2. Study area

The Gulf of Ancud and the Comau Fjord are part of the Andean landscape, with marked tectonic, volcanic, and glacial activity and climatic-environmental changes from the Pleistocene era to the present. The Comau Fjord is located between the mouth of the rivers/fjords Quintupeu and Vodudahue, covering a distance approximately 24 km long, with a maximum and minimum width of 11 and 2 km, respectively. The flanks of the fjord have a steep gradient (>30°) with heights that reach above 1000 m.a.s.l. (**Figure 1**).

Furthermore, the Comau Fjord area is scarcely populated (300 inhabitants during the year) with an incipient aquaculture industry oriented to large international markets. The area's connectivity is poor, with access only by sea (private and with State subsidy). Nevertheless the construction of a highway on the fjord's eastern flank is projected and currently under design that could stimulate development of the local and regional economy. Because of the incipient aquaculture industry in the fjord, an increase in population and economic activities in the area can be projected, but these activities will be located in an area with threats of natural hydro-meteorological, seismic-tectonic and oceanographic events of an Andean Patagonian fjord with a meso-tidal regime.
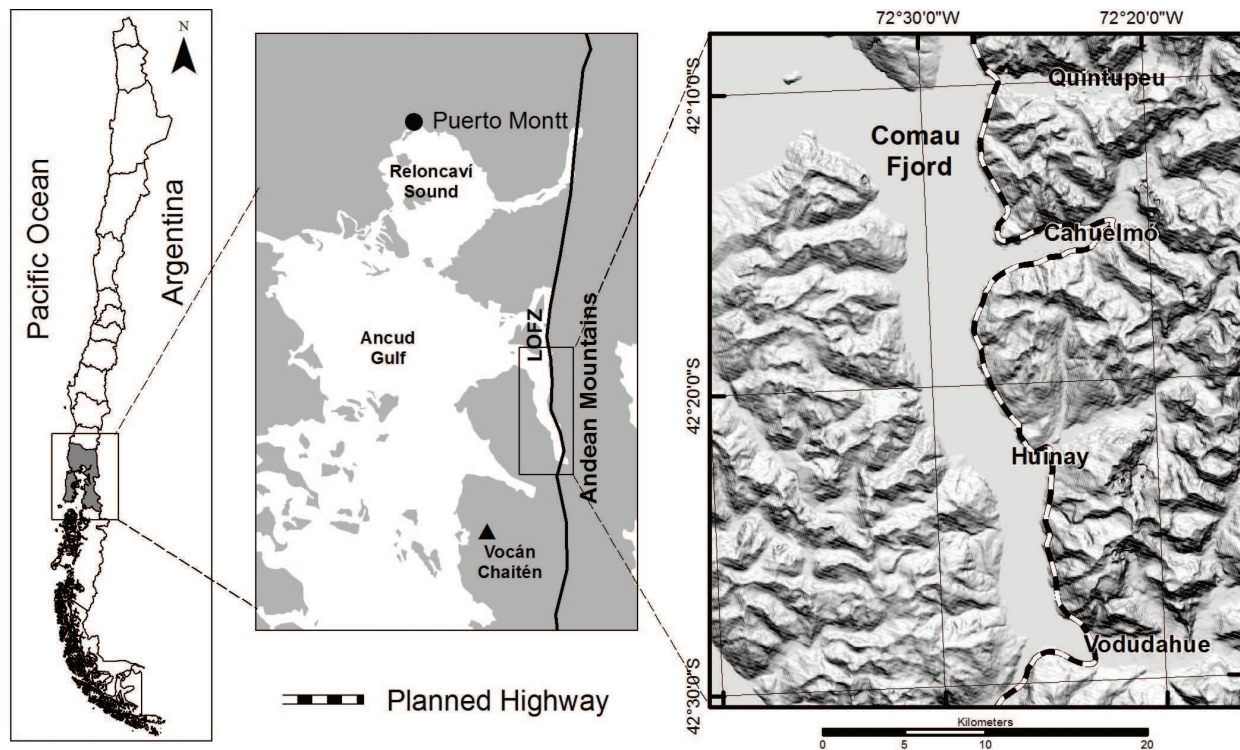
Figure 1. Study area.

The Comau Fjord is located directly on the Liquiñe-Ofqui Fault Zone (LOFZ, **Figures 1** and **2**), a regional fault system parallel to the Nazca and South American tectonic plate boundary, with activity during the late Cenozoic era [28, 29]. The LOFZ is a seismically active fault system [28, 29] in Chile's Northern Patagonia, which in 2007 generated a seismic swarm in the Aysén Fjord (45°25′S/72°581′W), with a principal earthquake (Mw 6.2), landslides and tsunamis. The tsunami wave reached 10 m [30–32]. The Chaitén Volcano (42°50′S/72°32′W) is also associated with the LOFZ. The volcano experienced a significant eruption in 2008 [33], and its ash was identified in the zone of Comau (**Figure 1**).

Though detailed geological studies of the area are not available, the geological map of [34] shows that the predominant lithological units are Jurassic intrusions (diorites, gabbros, monzodiorites), metamorphic rocks of schist with amphibolitic characteristics of the Paleozoic era and Quaternary volcanic rock.

Climatically, the region is subjected to winds from the west and the alternating cold front systems associated with a subpolar low-pressure zone, creating temperate oceanic and subpolar climates [35]. Extreme climate scenarios, from the most optimistic to the most severe (B2 and A1F1) of the IPCC [36] suggest that at the end of the twenty-first century (1971–2100) there will be a notable advance of Mediterranean climates with mild summers as far south as 46°S [37], while maintaining a zone of a more oceanic climate type (Cfb). Sarricolea and Figueroa [38] show precipitation diminishing by more than 200 mm and temperatures increasing up to 4°C of average annual temperature until the end of the twenty-first century. Using all models of the AR5 for precipitation and temperature, the following information was obtained:
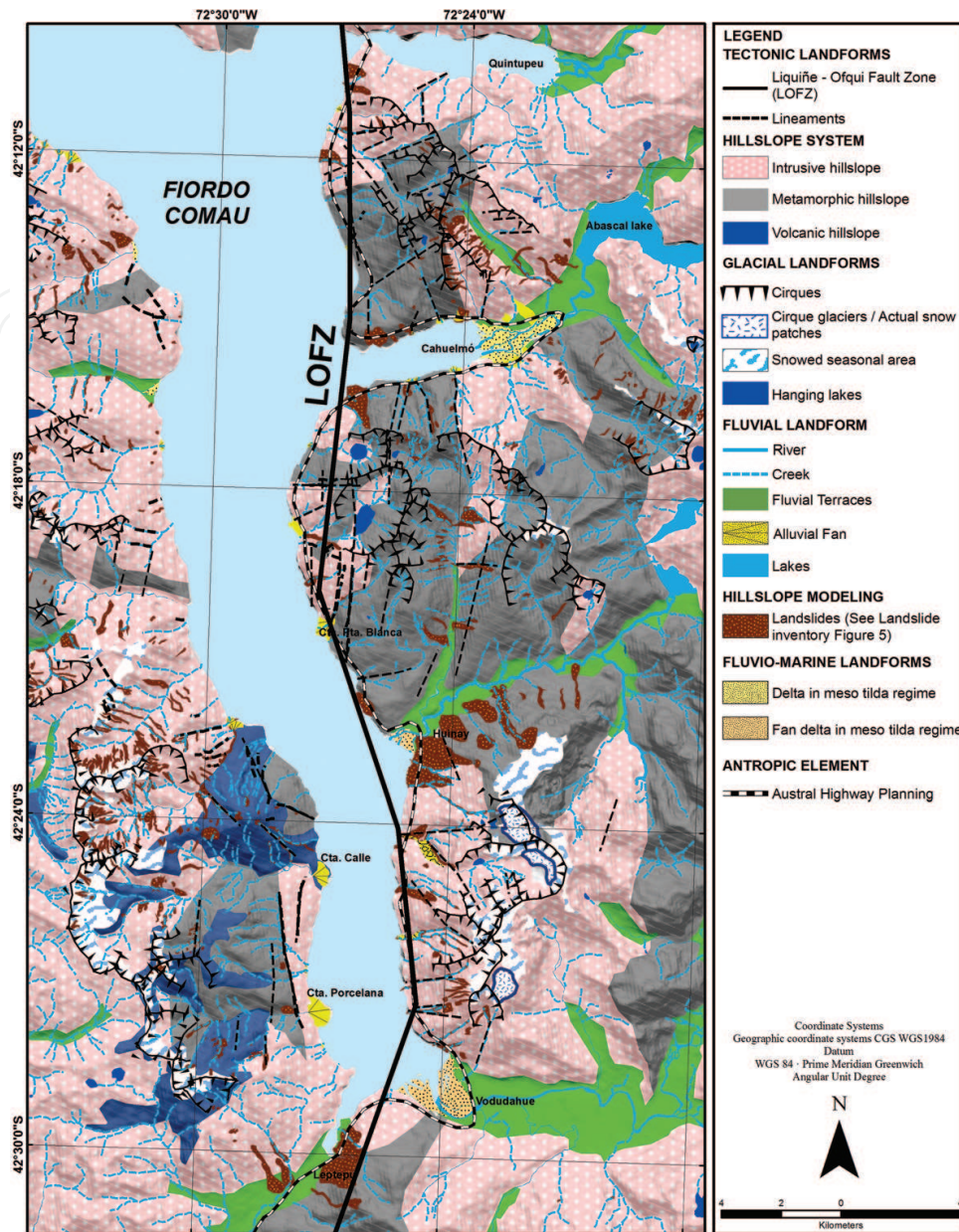
Figure 2. Geomorphological map with an inventory of landslides, glaciers and hanging lakes.

The temperature will increase in the RCP 2.6 and RCP 8.5 scenarios in the same way until 2020. Subsequently in the RCP 2.6 scenario (and until the end of the twenty-first century), temperatures will establish 1.5°C above the average temperatures for the twentieth century. While the RCP 8.5 continues increasing until the end of the twenty-first century with temperatures 3.7°C above those registered in the twentieth century.

Precipitation does not show significant differences between the RCP 2.5 and RCP 8.5 scenarios until 2050, but toward the end of the twenty-first century, the RCP 2.6 maintains the amounts of precipitation, while the RCP 8.5 decreases by 200 mm.

3. Methodology

The methodological focus was based on the geomorphology and GIS processes carried out to establish the natural hazard conditions using the following scheme:
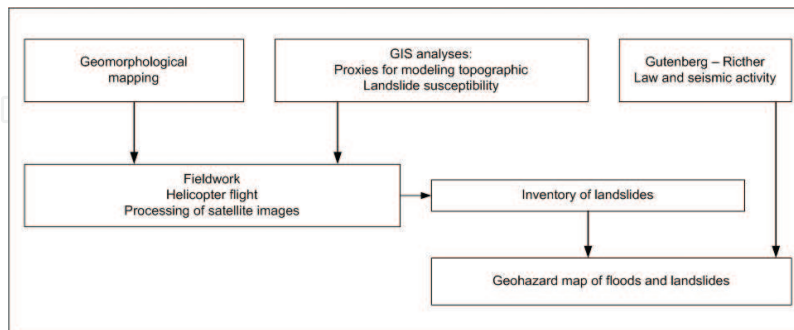
Geomorphological mapping: This was undertaken by means of aerial photograph interpretation and complemented with the geological map at scale 1:250,000 [34]. Due to difficult access to the study area, the high slope angle and elevation of both sides of the fjord, boat and helicopter access were used to examine landforms and validate the geomorphological mapping. The fieldwork was done in January and May 2016 and February 2017. A geomorphological classification for Andean cordillera environments was used [39], combined with lithology and morpho-structure [40]. Furthermore, an inventory of the fjord's hanging lakes and glaciers was completed.

GIS and proxies for modeling topographic indexes: The methodology of Märker et al. [41–43] was used to elaborate a high resolution Digital Elevation Model (DEM) (Alos/Prism 10 m o SRTM 25x) hydrologically corrected according to the Planchón and Darboux algorithm [44], reprocessed for analysis of terrain using SAGA GIS. Processes of hydrological erosion were modeled applying the following indexes: the Stream Power Index (SPI), the Transport Capacity Index (TCI) and the Topographic Wetness Index (TWI). The SPI was used to identify susceptibility to erosion and transport of sediments frequently accumulated in turbulent flows. This model describes the effects of the processes of fluvial lineal erosion and stream incisions, such as gullies, ravines and lateral erosion of beds. The Transport Capacity Index (TCI) was used to indicate areas prone to laminar erosion, sediment transport and processes of deposition. The Topographic Wetness Index (TWI) provides information on the accumulation of water and soil saturation around flat terrain units or topographical depressions, suggesting processes of surface runoff with substrate saturation and areas susceptible to flooding. This index was used to estimate inundation zones along fluvial riverbeds and ravines. Furthermore, modeling of topographical data using GIS tools was carried out to complement the geomorphological analysis, especially for those parts of the mountain on which fieldwork could not be done.

Landslide inventory: A photointerpretation of aerial photographs (1982, 1997, 1:20,000 and 1:70,000) and Google Earth was completed and validated by fieldwork. Landslides were

identified by morphological evidence, according to the criteria of Náquira [45], Sepúlveda and Serey [30] and Sepúlveda et al. [32–47] for fjord environments. Vegetated landslides were also identified that occurred in the past but at unknown dates.

Landslide susceptibility: The analysis of landslide susceptibility was carried out using the bivariate statistical analysis of Van Westen [48], applied by Molina [49], using as variables the gradient, orientation and height of the hillslope, curvature and profile, distance to the drainage networks and to the faults, density of drainage and faults/lineations, and the lithological units as evidence of geomorphological, hydrologic and geological characteristics of the fjord. The method requires a landslide inventory. The landslide susceptibility map was developed using weighing factors according to the method of Dahal et al. [50], dividing the factors in representative classes of the study area and intersecting with the inventory results. Weights were assigned as a function of landslide density found in each pixel factor. The ranges were reclassified for the study zone by Náquira [45] as high susceptibility, with 35% of the highest weighted values; moderate susceptibility, represented between 35 and 62%; and low susceptibility, between 62 and 100% of the weight [49].

Gutenberg-Richter Law and seismic activity: This was used to identify seismic interplate continental or cortical events occurring in the area (41°27′- 43°30′S), according to the data from the USGS in the period 1919–2016. The model connects the frequency and the magnitude of earthquakes [51]. This information is used only as an indicator of recurrent superficial seismic activity associated with the LOFZ and as a potential trigger for landslides and tsunamis.

The results of the Geohazard map are subject to uncertainty given the variability of precipitation and temperature in a climate change scenario, which was not modeled in this study.

4. Results and discussion

4.1. Geomorphological mapping

The geomorphological map shows a predominance of hillslopes of metamorphic and plutonic rock [52] that have been classified as active slopes because of the strong lineal incision, the presence of free-faces with several discontinuities such as joints, faults and fractures creating planes of weakness around rocky slopes in the zone of seasonal nivation, and the presence of talus, covered by dense vegetation of *Pilgerodendron uviferum*, with slopes above 30° (the altitude limit of vegetation has been identified as 1000 m.a.s.l.). A slope classification according to thresholds of morphogenetic processes (**Table 1**) was applied demonstrating that 61% have a 20°–30° slope and more than 45° of incline. Such measures favor processes of slope dynamics by gravitational effect, which are further favored by the high rainfall distributed throughout the year (5000 mm/year).

Numerous individual cirques and systems of coalesced cirques on both flanks of the fjord are the inherited forms of glacial excavation. The flanks' altitudinal slopes oscillate between ~600 and ~1000 m.a.s.l. (**Figure 2**) with respect to the base of the fjord. Landforms indicating active

hillslope instability are debris cones and localized slopes at the base of the cirques as well as on the hillslopes of the fjord.

Relevant factors of geomorphology are the numerous fractures and structural lineaments related with the LOZF that are identified in the granite, metamorphic and volcanic rock (**Figure 2**). These factors were incorporated in landslide modeling.

With regards to alluvial processes, the geomorphological map (**Figure 2**) shows that alluvial fans on the riverbeds of the fjord are almost inexistent given that the gradient and morphology of the fjord are unfavorable for their development, except for three hydrographic basins, with surfaces over ~15km^2, that discharge on the western shore of the fjord. The size of these alluvial fans ranges from ~300 to ~750 m (i.e. linear distance from the apex to the distal zone). On the other hand, in the eastern zone of the fjord, macro tidal fan deltas have formed associated with the three principal Andean hydrographic basins of the Cahuelmó, Huinay and Vodudahue rivers. These are large alluvial fans in a macro tidal environment, formed by coalesced lobes of gravel [53], except for Cahuelmó, which is itself a delta, according to the predominant sandy sedimentology identified in fieldwork.

Eight hanging lakes were identified on the eastern flank of the fjord on steep slopes with dense native forests (**Figures 2** and **3**). These are systems of three and four interconnected lakes, filled

Slope	Area km^2	Area %
Horizontal (0°–2°)	3.96	1.63
Gentle (2.1°–5°)	3.96	1.62
Moderate (5.1°–10°)	10.81	4.43
Strong (10.1°–20°)	39.06	16.02
Very strong to moderately steep (20.1°–30°)	60.92	24.99
Steep (30.1°–45°)	88.74	36.39
Very steep (>45°)	36.4	14.93
		Total area km^2: 243.84

Table 1. Classification of slopes on the Comau fjord.
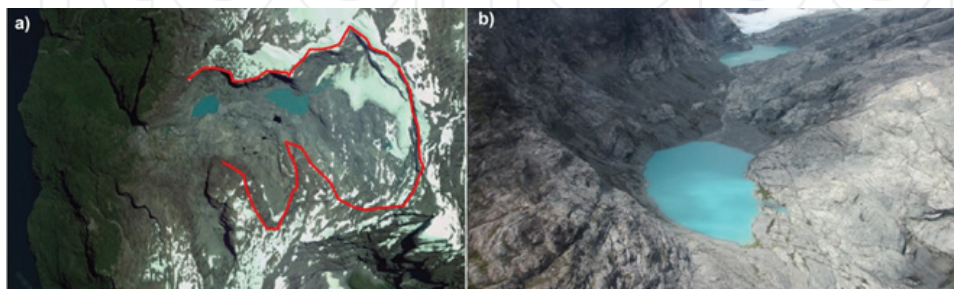

Figure 3. Hanging lakes. (a) Image showing the border of the cirque (red line) and two connected hanging lakes developed as the glacier retreats. (b) Lateral and oblique view of the hanging lakes on massive and fractured igneous rock, and glacier at the back.

by a fusion of glacial waters from the receding glacier identified in the last 30 years. These lakes are associated with glacier cirque, located between ~1200 and 1800 m.a.s.l., with a S-SE orientation. In the glacial lakes there are only rocky thresholds, without moraines; these glacial lakes supply water to the hanging falls. There is no glacial lake outburst floods (GLOF) observed.

4.2. GIS and proxies for modeling topographic indexes

The results showed that because of the steep gradient of Comau Fjord's western hillslope (slope > 45°), high levels of lineal erosion were generated, identified in **Figure 4A**. The areas with the most significant processes of lineal erosion (red) are principally associated with stream incisions developed on the granite and metamorphic rock slopes with structural lineaments to which are associated the ravines that connect the cirque glaciers and the hanging lakes. In addition, these ravines dissect the fjord walls, permitting the transfer of runoff and detritus from the cirques up to the fjord's base. The fluvial valleys of the Vodudahue, Huinay and Cahuelmó present elevated ranges of lineal and lateral erosion, associated with the development of a drainage network of glacial and periglacial Andean catchment areas. By contrast, areas with low SPI show good agreement with ridges of divides and fluvial plains, where the slope tends to be lower than 5°.

The results of the Transport Capacity Index (TCI), in **Figure 4B** shows the marked influence of the gradient on the slopes and the adjacent valleys; these are areas that present the surfaces most affected by laminar erosion (red colors). These areas show evidence of landslides and talus in the slopes, as a response to the high susceptibility to the soil erosion of the hillslopes. The red lines on the bottom of the valley and ravines show the action of the water. There are marked incisions in the ravines and streams, many of which come from glacier-lake or fluvial valley systems, with distal deposits, alluvial fans or fan deltas. Just as with SPI, areas with low TCI are associated with fluvial plains and fjord divides.
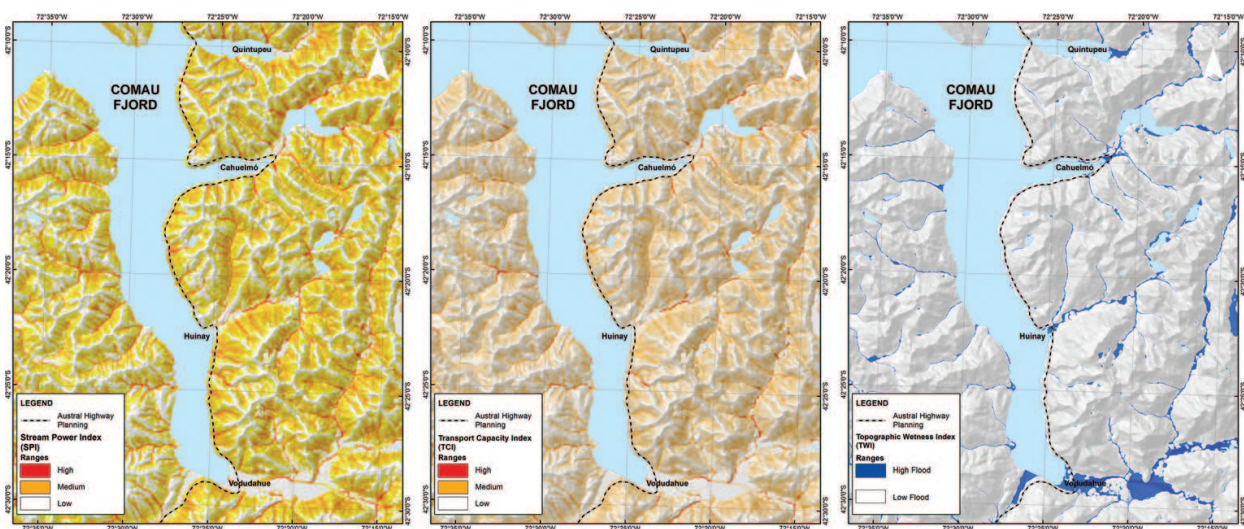

Figure 4. A. Stream Power Index (SPI), B. Transport Capacity Index (TCI), C. Topographic Wetness Index (TWI).

The Topographic Wetness Index (TWI), as can be seen in **Figure 4C**, shows areas with the highest potential of water accumulation are the valley bottoms of the principal catchment basins (Cahuelmo, Huinay, Vododahué), where the low fluvial terraces (**Figure 2**) present flood risk. The TWI results in the study area clearly indicate the presence of hanging lakes and cirque glaciers. The western slope of the fjord presents scarce areas of water accumulation because of the steepness of its slope, but a moderate potential for saturation that can be associated with areas prone to landslides. The results of the index's application were validated in fieldwork by helicopter flight.

5. Geohazards: landslide and floods

The model of landslide susceptibility shown in **Figure 5** demonstrates high susceptibility on the eastern side of the fjord, which can be associated with steep slopes of metamorphic and igneous rock, a factor that Oppikofer et al. [27], Blikra et al. [25] indicate as highly favorable for this type of phenomena. The model included the density of structural lineaments (faults) and lakes, which contribute to the propensity to landsliding in the eastern zone.

Figure 5 also shows the location of debris flows, which show spatial agreement with the SPI and the TCI (**Figure 4**), associated with hydrologic action in micro catchment areas and ravines. On the eastern hillslope, the presence of receding glaciers and their associated lakes constitute potential areas for debris flows. There are also a large number of coalesced cirque glaciers. Consequently, the results of landslide susceptibility, geomorphology and GIS Index coincide.

The rock fall features cover large sections of the slopes as evidence of geological processes that have been masked by the vegetation of the austral forest and demonstrate probable synergic action of the LOZF's tectonic action (**Figure 6A** and **B**). The predominant forms are earth and rock slides, observed as much of plutonic as of metamorphic rock (**Figure 6C** and **D**). Many landslides were found to be covered by vegetation, principally ferns, pioneer vegetation that date from an indeterminate time in the past (**Figure 6E**); *P. uviferum* forests take decades to grow and up to 200 years to reach adult size (These forms were classified in the inventory as vegetated earth and rock slide and supply the principal evidence of dynamic processes on the slopes of the fjord. On the slopes associated with volcanic rock, above all on the western side, rocks and earth slides predominate (**Figure 6F**).

The debris flows identified do not present a pattern associated with a specific type of rock, rather they are associated with ravines and streams in micro catchments (**Figure 7**) and glacial retreat catchments.

Areas subjected to fluvial inundation are identified in the mid and lower sections of the principal valley and sub-catchment area tributaries (**Figure 5**). The morphology of fluvial terraces eroded by historic fluvial rises is evidence of this activity, above all in the most distal parts where the Holocene fluvial terraces still present evidence of seasonal fluvial action
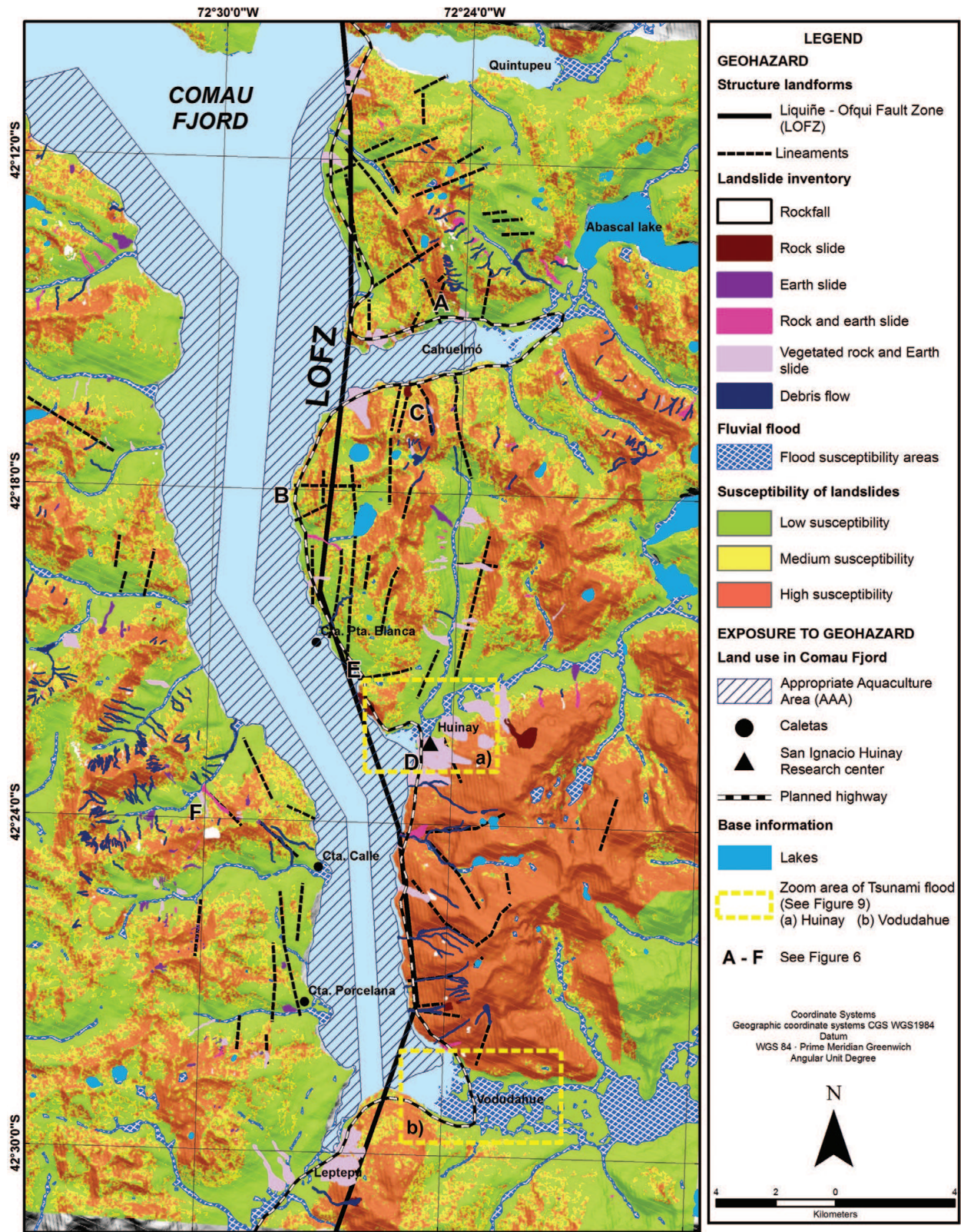
Figure 5. Geohazard map: landslide susceptibility and inventory, rivers and tsunami flood areas.

(**Figures 5** and **7**). The fan delta morphology (**Figure 8**) that drains the principal valleys also shows evidence of flooding due to tidal changes. The results of the TWI (**Figure 4**) permitted analysis of areas difficult to access, and these results were also validated by helicopter flight in January 2016.
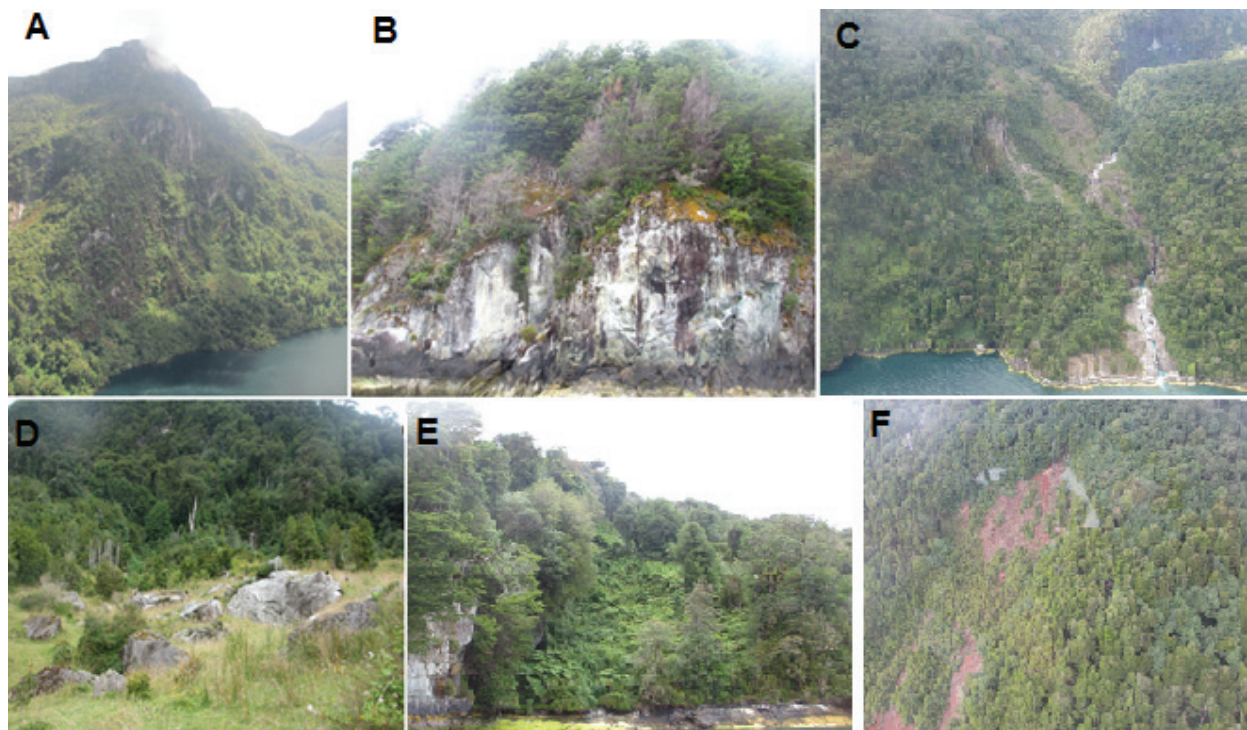

Figure 6. Inventory of landslides. A–B: vegetated rock fall area and present day rock fall feature. C: earth and rockslides on the eastern side of fjord. D: the lower deposits associated to the great event occurred in 1957. E: vegetated earth and rockslide. F: rocks and earth (soil) slides on volcanic slopes (See location of the photos in **Figure 5**).

Figure 7. Oblique view of the Vodudahue river valley showing low alluvial terraces prone to flooding, which corresponds to areas with high Topographic Wetness Index (TWI). On the right side of the figure a fan delta is shown with a meso-tidal regime in contact with the fjord. The figure also shows granitic and vegetated hillslopes that border both sides of the valley. Source: Photography taken by the authors during helicopter flight.
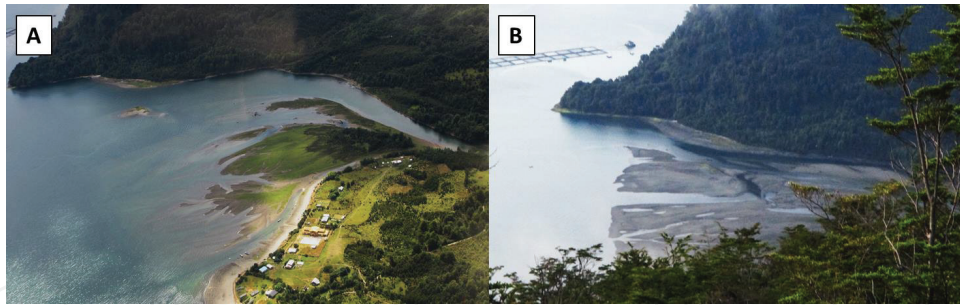
Figure 8. Fan delta and changes of tide in Huinay river outlet (A) High tide, January 28 (15:30 hrs.), (B) Low tide, January 22 (20:32 hrs.). Source: González [54].
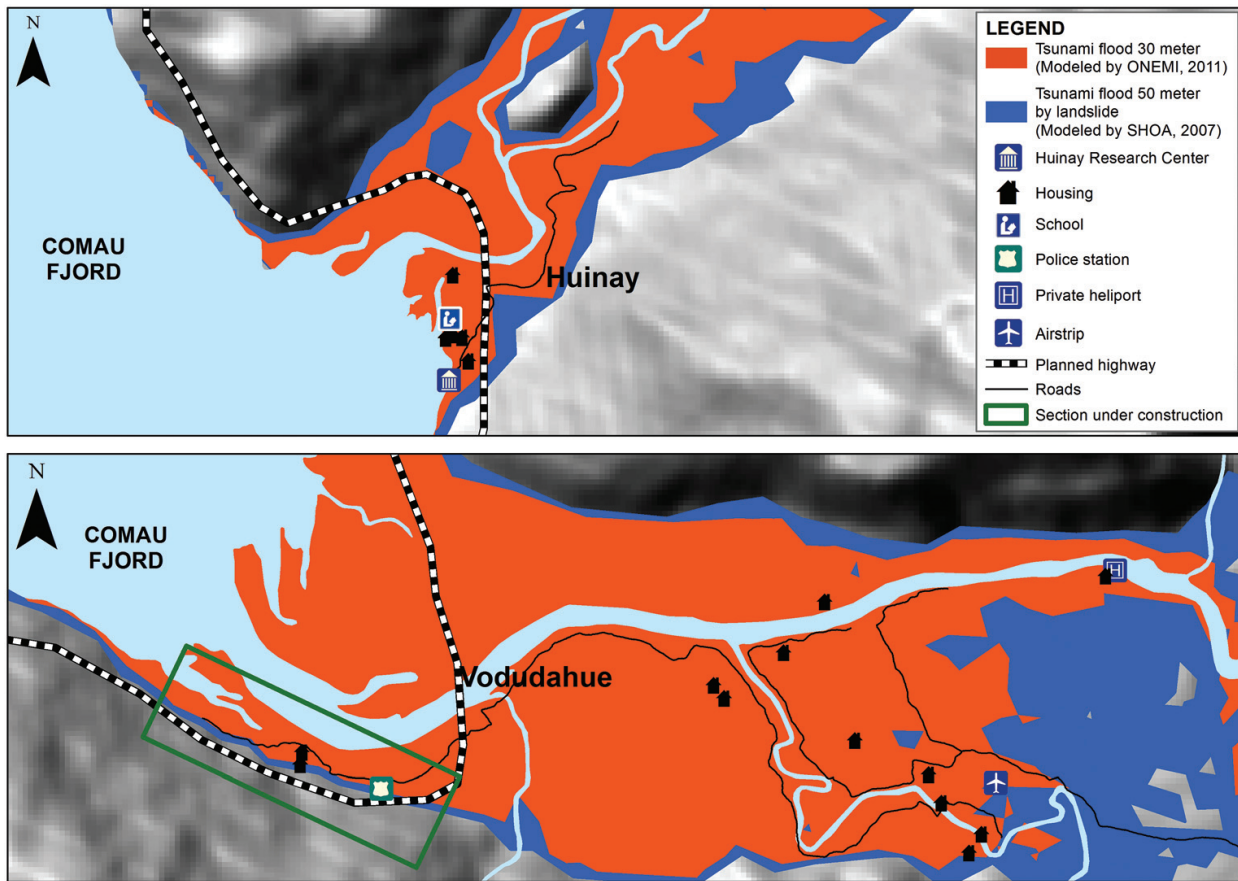

Figure 9. Areas of potential flooding by tsunamis. The low lands with current and projected uses would be the most vulnerable.

6. Seismic activity and landslide-tsunami trigger

Results of the calculation of seismic susceptibility using the Gutenberg-Richter Law, identified 16 intraplate continental seismic events in the 97 years analyzed (**Table 2**). Cortical earthquakes correspond to 14% of the total events. Though the coefficient of correlation between

Gutenberg-Richter Law

Type of seismic event	N° de seismic events	Magnitude		Depth		Coefficient of lineal regression	
		Min.	Max.	Min.	Max.	a	b
Complete register	142	2.9	7.2	0	165.4	5.012	−0.670
Intraplate continental seismic events	16	3	7.2	7.8	36.2	2.859	−0.440
Interplate seismic events	85	3.4	7	7.8	47.5	4.674	−0.631
Intraplate oceanic seismic events	13	3.9	6	52.2	165.4	3.505	−0.585
Volcanic seismic events	28	2.9	5.2	0	10	8.539	−1.655

Table 2. Parameters of the Gutenberg-Richter Law (Log N = a + bM, where N is number of earthquakes and M the magnitude) for seismic activity 1919–2016.

the regression analysis and the data is low (0.83), and does not allow for quantifying the return period, a recurrent condition of seismic activity in the LOFZ can be established. Furthermore, this activity is a factor in the geohazard of landslips and tsunamis, as evidenced by Sepúlveda et al. [32] in the Aysén Fjord.

In the context of potential activation of seismic activity that could generate a tsunami, a map was created with areas affected by flooding, adding three wave heights, according to the standards of the State of Chile and the known event that occurred in the Aysén Fjord in 2007.

Figure 9 shows the areas that are potentially susceptible and vulnerable to flooding by tsunami. The State of Chile has defined 30 m above sea level as the safety zone [55]; the wave height of 50 m is the maximum level modeled for the Aysén Fjord [56]. To this level, 7 additional meters must be added from high tide as a worst-case scenario.

The risk of landslides in fjords has been studied in the northern hemisphere because of its impact on human life and economic loss [26, 27, 57], but in Chile the region of the fjords constitutes an isolated territory uncoupled from the urban-regional-national system, unpopulated and lacking infrastructure [6].

This situation is in the process of changing with the construction of a land route to foment inter-regional integration. The route is projected to benefit the growth of the aquaculture industry, above all for the export of salmon and the development of economic activity in the valleys of the Huinay and Vodudahue, where small settlements already exist (**Figure 9**). The case of the Vodudahue is more complex because the valley is quite wide, apt for forestry, livestock and farming, and has internal roads to connect to the route under construction (CH 7), that will connect to the port, continental Chile and South Patagonia. Fishing lodges and an ecotourism industry are being constructed for an elite socio-economic international market.

7. Conclusions

The predominant feature of Comau Fjord's geomorphological setting is its steeply graded hillslopes, 36% of its territory in thresholds above 30° (61% have a 20°–30° slope and more than 45° of incline), in addition to fractured intrusive and metamorphic rocks, most of them classified as free-faces and talus landforms, above all on its higher eastern flank. The talus are vegetated providing evidence of a timberline 1000 m.a.s.l., above which are bare rocks exposed to glacial rainfall activity, and processes of nivation. The presence of vegetated talus on both sides of the fjord is a constant, as are the numerous ravines because of intense precipitation and glacial melting activity in the fjord.

The landslide inventory performed in fieldwork is geomorphic evidence of the dynamic processes acting on the hillslopes. The landslide susceptibility modeled for the study area, based methodologically on the inventory and statistical analysis, strongly suggests that the study area shows conditions for landsliding. Furthermore, the seismic activity identified for this zone as part of the influence of the LOZF was described based on the magnitude-frequency relationships using the Gutenberg-Richter Law. Although results show a low coefficient of linear regressions (-0.4) for cortical seismic activity near the study area, this can be considered as another latent trigger for landslides and tsunamis. Historical reports, in fact, have documented the triggering of landsliding inducing tsunamis in Aysen 2007.

GIS modeling of topographic indexes is an important methodological tool for geomorphological terrain analysis in areas with difficult access to the Andean fjords and catchment areas of the Chilean Patagonia. This tool has been useful to show areas prone to be flooded and zones with landslide susceptibility.

The zone's climatic conditions of very high rainfall (5000 mm/year), together with the presence of low alluvial terraces, favor the dynamic processes that generate fluvial flooding. Identification of areas of fluvial flooding is associated with high annual rainfall and a winter peak level, but also with the increase in spring and summer temperatures that contribute to the receding nature of the Andean glaciers, and the increasing river flow. The trend of climatic change in the zone is set to continue throughout this century. Identified areas of fluvial flooding correspond to the Holocene terraces, currently not in use. The projected highway in the fluvial valleys will be affected by this threat.

The construction of Route CH 7 will be a strong incentive for economic activity in the fjord area, principally in aquaculture and tourism. As shown in the geomorphological and geohazards maps (**Figures 2**, **5**, and **9**), most of the planned highway that will be built at the eastern base of the fjord can be disrupted by rock falls, rock and earth slides and debris flows. Indeed, at least 24 critical zones of exposure can be identified on the hazard maps. Moreover, areas that currently have human settlements are located on geomorphological units such us low alluvial terraces and deltas, prone to flooding. These economic activities will, thus, be exposed and vulnerable to future risks given the identified geohazards. For this reason, direct or indirect mitigation controls such as land use planning should be considered to reduce the risk of disaster at the study site.

Acknowledgements

Author details

María-Victoria Soto[1,2]*, Pablo Sarricolea[1,2], Sergio A. Sepúlveda[2,3,4], Misael Cabello[5], Ignacio Ibarra[1], Constanza Molina[3] and Michael Maerker[6]

*Address all correspondence to: mvsoto@uchilefau.cl

1 Department of Geography, University of Chile, Santiago, Chile

2 CITRID, Risk Reduction And Disaster Program, University of Chile, Chile

3 Department of Geology, University of Chile, Santiago, Chile

4 Institute of Engineering Sciences, University of O'Higgins, Rancagua, Chile

5 Physical Geography Lab. Department of Geography, University of Chile, Chile

6 Department of Earth and Environmental Sciences, University of Pavia, Italy

References

[1] Soto MV, Moreno R. Implicancias del crecimiento urbano en el piedmont andino de Santiago: un tema de sustentabilidad urbana. Chile. En: Sobre la medición de la forma del espacio urbano: Aplicación a Santiago (Chile) y Zaragoza (España). 2011;**XX**:86-95

[2] Holsten A, Kropp JP. An integrated and transferable climate change vulnerability assessment for regional application. Natural Hazards. 2012;**64**(3):1977-1999

[3] Sahin O, Mohamed S. Coastal vulnerability to sea-level rise: a spatial–temporal assessment framework. Natural Hazards. 2014;**70**(1):395-414. DOI: 10.1007/s11069-013-0818-4

[4] Castro CP, Ibarra I, Lukas M, Sarmiento JP. Disaster risk construction in the progressive consolidation of informal settlements: Iquique and Puerto Montt (Chile) case studied. International Journal of Disaster Risk Reduction. 2015;**13**:109-127. DOI: 10.1016/j.ijdrr.2015.05.001

[5] Ibarra I, Castro CP, Soto MV, Rauld R. Applied Geomorphology to assessment of natural hazards at the southern area of Pichilemu district, O'Higgins Region, Chile. Revista Investigaciones Geográficas. 2016;**51**:61-80. DOI: 10.5354/0719-5370.2016.42521

[6] Soto MV, Arratia P, Cabello M, Moreno R, Whyndam K. Amenazas de origen natural y exposición de obras de conectividad estratégica en territorios extremos. Fiordo Comau, Norpatagonia de Chile. Revista de Geografía Norte Grande. 2018. Article accepted, in press

[7] Cardona OD. Teoría del Riesgos y Desastres. En: Gestión Integral de Riesgos y Desastres. Curso de Educación Superior. Universidad Internacional de Florida 2009 Inédito

[8] Aubrecht C, Fuchs S, Neuhold C. Spatio-temporal aspects and dimensions in integrated disaster risk management. Natural Hazards. 2013;**68**:1205-1216. DOI: 10.1007/s11069-013-0619-9

[9] Lei Y, Wang J. A preliminary discussion on the opportunities and challenges of linking climate change adaptation with disaster risk reduction. Natural Hazards. 2014;**71**(3):1587-1597. DOI: 10.1007/s11069-013-0966-6

[10] List G, Coomes OT. Natural hazards and risk in rice cultivation along the upper Amazon River. Natural Hazards. 2017;**87**(1):165-184. DOI: 10.1007/s11069-017-2758-x

[11] Schmidt-Thomé P. Towards Applying Climate Change Adaptation, 49-60. Investigaciones Geográficas. 2017;**67**:45-60. DOI: 10.14198/INGEO2017.67.03

[12] Banks JC, Camp JV, Abkowitz MD. Adaptation planning for floods: a review of available tools. Natural Hazards. 2014;**70**:1327-1337. DOI: 10.1007/s11069-013-0876-7

[13] Soto MV, Sarricolea P, Sepúlveda SA, Rodolfi G, Cabello M, Maerker M. Assessment of hydro-geomorphological hazard potentials in the Chilean semiarid coastal range and its impacts on La Serena city, Coquimbo Region. Natural Hazards. 2017;**88**(1):431-452. DOI: 10.1007/s11069-017-2873-8

[14] Kappes MS, Gruber K, Frigerio S, Bell R, Keiler M, Glade T. The Multi Risk platform: the technical concept and application of a regional-scale multi hazards exposure analysis tool. Geomorphology. 2012;**151-152**:139-155. DOI: 10.1016/j.geomorph.2012.01.024

[15] Keiler M, Kellerer-Pirkbauer A, Otto JC. Concepts and implications of environmental change and human impact: studies from Austrian geomorphological. Geografiska Annaler. Serie A. Physical Geography. 2012;**94**:1-5. DOI: 10.1111/j.1468-0459.2012.00457.x

[16] Beniston M, Stoffel M, Hill M (eds). ACQWA. Assessing climate impacts on the quantity and quality of water. The EU/FP7 ACQWA Project Science and Policy Brief. A large integrating Project under EU R&D Framework Programme 7 (FP7). Université de Genéve. 2013. p. 98

[17] Janke J, Bellisario A, Ferrando F. Classification of debris-covered glaciers and rock glaciers in the Andes of central Chile. Geomorphology. 2015;**241**:98-121. DOI: 10.1016/j.geomorph.2015.03.034

[18] Comisión Nacional de Medio Ambiente (CONAMA). Estudio de la variabilidad climática en Chile para el siglo XXI. En: Informe Final. Realizado por el Departamento de Geofísica, Universidad de Chile. 2006. p. 71

[19] Garreaud R, Barichivich J, Christie DA, Maldonado A. Interannual variability of the coastal fog at Fray Jorge relict forests in semiarid Chile. Journal of Geophysical Research, Biogeosciences. 2008;**113**(G04011). DOI: 10.1029/2008JG000709

[20] Pino P, Iglesias V, Garreaud R, Cortés S, Canals M, Folch W, Burgos S, Levy K. Naechar. L., Steenland, K. Chile confronts its environmental future under uncertain perspectives of climate change. Annals of Global Health. 2015;**81**(3):354-367

[21] Sarricolea P, Herrera-Ossandon MJ, Meseguer-Ruiz O. Climatic regionalization of continental Chile. Journal of Maps. 2017;**13**:66-74. DOI: 10.1080/17445647.2016.1259592

[22] Wilcox BP, Sorice MG, Young MH. Dryland ecohydrology in the anthropocene: Taking stock of human–ecological interactions. Geography Compass. 2011;**5**(3):112-127. DOI: 10.1111/j.1749-8198.2011.00413.x

[23] Williams M, Zalasiewicz J, Waters C, Edgeworth M, Bennett C, Barnosky A, Ellis E, Ellis M, Cearreta A, Haff P, Ivar do Sul J, Leinfelder R, McNeill J, Odada E, Oreskes N, Revkin A, Richter D, Steffen W, Summerhayes C, Syvitski J, Vidas D, Wagreich M, Wing S, Wolfe A, Zhisheng A. The anthropocene: A conspicuous stratigraphical signal of anthropogenic changes in production and consumption across the biosphere. Earth's Future. 2016;**4**(3): 34-53. DOI: 10.1002/2015EF000339

[24] Barton JR, Irarrázaval F. Adaptación al cambio climático y gestión de riesgos naturales: buscando síntesis en la planificación urbana. Revista de Geografía Norte Grande. 2016;**63**:87-110. DOI: 10.4067/S0718-34022016000100006

[25] Blikra LH, Longva O, Braathen A, Anda E, Dehls JF, Stalsberg K. Rock slope failures in Norwegian fjord areas: Examples, spatial distribution and temporal pattern. In: Landslides from Massive Rock Slope Failure. Dordrecht: Springer; 2006;**49**:475-496. DOI: 10.1007/978-1-4020-4037-5_26

[26] Lacasse S, Eidsvik U, Nadim F, Hoeg K, Blikra LH. Event tree analysis of Åknes rock slide hazard. In: 4th Canadian Conference on Geohazards, Université Laval. 2008, May. pp. 20-24

[27] Oppikofer T, Jaboyedoff M, Blikra L, Derron MH, Metzger R. Characterization and monitoring of the Åknes rockslide using terrestrial laser scanning. Natural Hazards and Earth System Sciences. 2009;**9**(3):1003-1019. DOI: 10.5194/nhess-9-1003-2009, 2009

[28] Vargas G, Rebolledo S, Sepúlveda SA, Lahsen A, Thiele R, Townley B, Lara M. Submarine earthquake rupture, active faulting and volcanism along the major Liquiñe-Ofqui Fault Zone and implications for seismic hazard assessment in the Patagonian Andes. Andean Geology. 2013;**40**(1). DOI: 10.5027/andgeoV40n1-a07

[29] Hervé F, Fuentes F, Calderón M, Fanning M, Quezada P, Pankhurst R, Rapela C. Ultramafic rocks in the North Patagonian Andes: Is their emplacement associated with the Neogene tectonics of the Liquiñe-Ofqui Fault Zone? Andean Geology. 2017;**44**(1):1-16. DOI: 10.5027/andgeoV44n1-a01

[30] Sepúlveda SA, Serey A. Tsunamigenic, earthquake-triggered rock slope failures during the April 21, 2007 Aisén earthquake, southern Chile (45.5° S). Andean Geology. 2010;**36**(1): 131-136. DOI: 10.5027/andgeoV36n1-a10

[31] Naranjo JA, Arenas M, Clavero J, Muñoz O. Mass movement-induced tsunamis: main effects during the Patagonian Fjordland seismic crisis in Aisén (45° 25'S), Chile. Andean Geology. 2009;**36**(1). DOI: 10.4067/S0718-71062009000100011

[32] Sepúlveda SA, Serey A, Lara M, Pavez A, Rebolledo S. Landslides induced by the April 2007 Aysén fjord earthquake, Chilean Patagonia. Landslides. 2010;**7**(4):483-492. DOI: 10.1007/s10346-010-0203-2

[33] Lara LE. The 2008 eruption of the Chaitén Volcano, Chile: A preliminary report. Andean Geology. 2009;**36**(1):125-130. DOI: 10.5027/andgeoV36n1-a09

[34] SERNAGEOMIN-BRGM. Carta Metalogénica X Región sur. Servicio Nacional de Geología y Minería–Bureau de Recherches Géologiques et Minières. Informe Registrado IR-95-05. 1995. 4 Tomos, 10 Vols., 95

[35] Sarricolea P, Herrera-Ossandon M, Meseguer-Ruiz Ó. Climatic regionalisation of continental Chile. Journal of Maps. 2017;**13**(2):66-73. DOI: 10.1080/17445647.2016.1259592

[36] IPCC. Climate Change: The Physical Science Basis. Contribution of Working Group I to the Fourth Assessment Report of the Intergovernmental Panel on Climate Change. Solomon S, Qin D, Manning M, Chen Z, Marquis M, Averyt KB, Miller HL, (eds.). Cambridge University Press, Cambridge, United Kingdom and New York, NY, USA, 2007. p. 996

[37] Rubel F, Kottek M. Observed and projected climate shifts 1901–2100 depicted by world maps of the Köppen-Geiger climate classification. Meteorologische Zeitschrift. 2010;**19**(2): 135-141. DOI: 10.1127/0941-2948/2010/0430

[38] Sarricolea P, Figueroa P. Pluviometría de los últimos 48 años en Chile centro-sur (33°40'-42°S) y sus patrones de variabilidad en el contexto de Cambio Climático Global. En XI Simposio Brasileiro de Climatología Geográfica. Curutiba Brasil. 2014. p. 10

[39] Araya-Vergara JF. Análisis de la carta geomorfológica de la Cuenca del Mapocho. Informaciones Geográficas. 1985;**32**:31-44. DOI: 10.5354/0719-5370.1985.27693

[40] Soto MV, Correa CP, Rodolfi G, Märker M, Torres RF, Torres RP, de Souza VR. Carta geomorfológica de la sección central y occidental de la Región Metropolitana de Santiago. Investigaciones Geográficas. 2007;**39**(91). DOI: 10.5354/0719-5370.2007.27763

[41] Märker M, Moretti S, Rodolfi G. Assessment of water erosion processes and dynamics in semi – arid regions of Southern Africa (kwazulu/Natal, RSA,and Swaziland) using the Erosion Response Units concept (ERU). Geografia Fisica e Dinamica Quaternaria. 2001;**24**:71-83

[42] Märker M, Castro CP, Pelacani S, Soto M-V. Assesment of degradation susceptibility in the Chacabuco Province of central using a morphometric based response units approach. Geografia Física e Dinamica Quaternaria. 2008;**31**:47-53

[43] Märker M, Pelacani S, Schröder BA. A Functional entity approach to predict soil erosion processes in a small Plio-Pleistocene Mediterranean catchment in Northern Chianti, Italy. Geomorphology. 2011;**125**(4):530-540. DOI: 10.1016/j.geomorph.2010.10.022

[44] Planchon O, Darboux F. A fast, simple and versatile algorithm to fill the depressions of digital elevation models. Catena. 2002;**46**(2):159-176. DOI: 10.1016/S0341-8162(01)00164-3

[45] Náquira V. Susceptibilidad remociones en masa en las costas de fiordos cercanos a Hornopirén, Memoria para optar al título de geóloga. Universidad de Chile. Facultad de Ciencias Físicas y Matemáticas. Santiago – Chile; 2009

[46] Sepúlveda SA, Náquira MV, Arenas M. Susceptibility of coastal landslides and related hazards in the Chilean Patagonia: The case of Hornopirén area (42°S). Investigaciones Geográficas. 2011;**43**:35-46. DOI: 10.5354/0719-5370.2011.18496

[47] Sepúlveda SA, Le Roux JP, Palma P. Application of the composite maps method for landslide susceptibility and its potential use for other natural risk analyses. Investigaciones Geográficas. 2013;**46**:47-56. DOI: 10.5354/0719-5370.2013.30282

[48] Van-Western CJ. Use of weights of evidence modelling for landslide susceptibility mapping lecture notes. International Institute for Geoinformation Science and Earth Observation (ITC), Enschede, The Netherlands. 2003. pp. 1-21

[49] Molina C. Análisis de susceptibilidad de remociones en masa en las costas del Fiordo Comau, X Región, Chile. Memoria para optar al grado de geológa. Universidad de Chile. Facultad de Ciencias Físicas y Matemáticas. Santiago – Chile; 2017

[50] Dahal RK, Hasegawa S, Nonomura A, Yamanaka M, Masuda T, Nishino K. GIS-based weights-of-evidence modelling of rainfall-induced landslides in small catchments for landslide susceptibility mapping. Environmental Geology. 2008;**54**(2):311-324. DOI: 10.1007/s00254-007-0818-3

[51] Nava FA, Márquez-Ramírez VH, Zúñiga FR, Lomnitz C. Gutenberg–Richter b-value determination and large-magnitudes sampling. Natural Hazards. 2017;**87**(1):1-11. DOI: 10.1007/s11069-017-2750-5

[52] Prian J. Síntesis geológica entre los 40°30'y 42°15' latitud sur. Parte centro-sur de la X Región, X Programa de Geocronología (monografías). Servicio Nacional de Geología y Minería (SERNAGEOMIN). 1994. p. 69

[53] Soto MV, González N.: Reconocimiento de formas deltaicas asociados a cuencas andinas en el Fiordo Comau: Fan deltas macromareales.Norpatagonia de Chile. IX Seminário Latino-americano e V Seminário Ibero-Americano de geografia física. Brasil; 2016. p. 12

[54] González N. Análisis y caracterización temporo-espacial de la morfología Fan-Delta en la localidad de Huinay, Fiordo Comau, región de Los Lagos. Memoria de título para optar al grado de Geógrafa. Facultad de Arquitectura y Urbanismo de la Universidad de Chile. Santiago – Chile. 2017

[55] ONEMI 2011 Oficina Nacional de Emergencia del Ministerio del Interior y Seguridad Pública (ONEMI).: Visor Chile preparado. Territorio y Amenazas http://geoportalonemi. maps.arcgis.com/apps/webappviewer/index.html?id=5062b40cc3e347c8b11fd8b20a639a88

[56] Servicio Hidrológico y Oceanográfico de la Armada. Puerto Aysén - Puerto Chacabuco. Carta de inundación por tsunami generado por remociones en masa. 2007. http://www. shoa.cl/servicios/citsu/pdf/citsu_aysen_low.pdf

[57] Anderson-Sköld Y, Bergman R, Jahansson M, Persson E, Nyberg L. Landslide risk management – A brief overview and example from Sweden of current situation and climate change. International Journal of Disaster Risk Reduction. 2013;**3**:44-61. DOI: 10.1016/j. ijdrr.2012.11.002